

Coherent acoustic oscillations of nanoscale Au triangles and pyramids: influence of size and substrate

R Taubert, F Hudert, A Bartels, F Merkt, A Habenicht, P Leiderer and T Dekorsy¹

Department of Physics and Center of Applied Photonics,
Universität Konstanz, D-78457 Konstanz, Germany
E-mail: thomas.dekorsy@uni-konstanz.de

New Journal of Physics **9** (2007) 376

Received 24 July 2007

Published 19 October 2007

Online at <http://www.njp.org/>

doi:10.1088/1367-2630/9/10/376

Abstract. We investigate the impulsively excited acoustic dynamics of nanoscale Au triangles of different sizes and thicknesses on silicon and glass substrates. We employ high-speed asynchronous optical sampling in order to study the damping of the acoustic vibrations with high sensitivity in the time domain. From the observed damping dynamics we deduce the reflection coefficient of acoustic energy from the gold–substrate interface. The observed damping times of coherent acoustic vibrations are found to be significantly longer than expected from the acoustic impedance mismatch for an ideal gold–substrate interface, hence pointing towards a reduced coupling strength. The strength of the coupling can be determined quantitatively. For Au triangles with large lateral size-to-thickness ratio, i.e. a small aspect ratio, the acoustic dynamics is dominated by a thickness oscillation similar to that of a closed film. For triangles with large aspect ratio the coherent acoustic excitation consists of a superposition of different three-dimensional modes which exhibit different damping times.

¹ Author to whom any correspondence should be addressed.

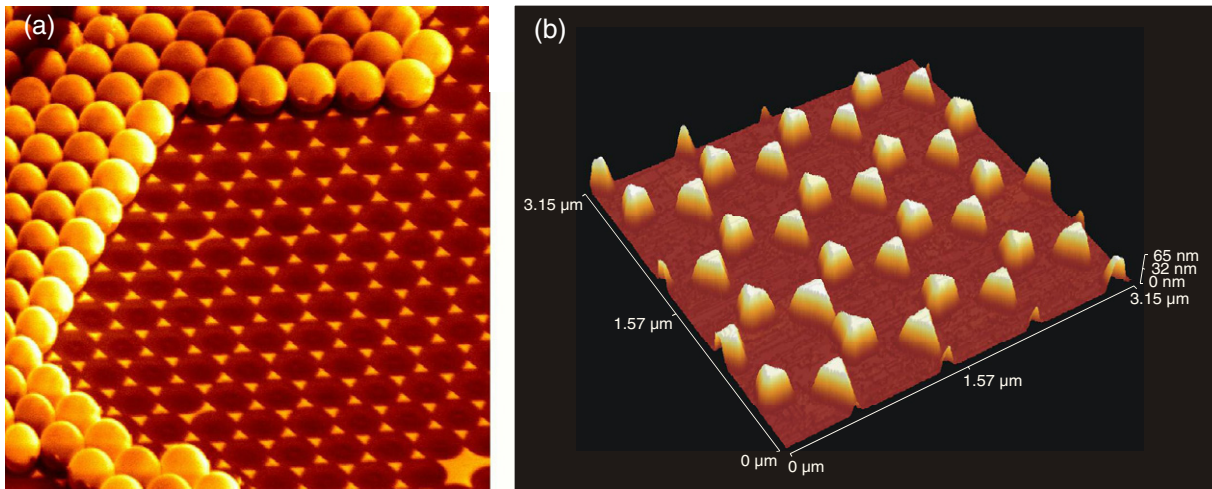


Figure 1. (a) Scanning electron microscope graph of Au triangles deposited on silicon. For the deposition process colloids of 800 nm have been used. (b) Atomic force microscope picture of Au triangles with 50 nm thickness.

The study of coherent acoustic vibrations of thin films and nanoscale objects is of importance for the understanding of heat flow on the nanometre length scale and on picosecond time scales ([1] and references therein). Picosecond ultrasound techniques based on sub-ps lasers are well established for the investigation of propagation, attenuation and damping of impulsively launched strain pulses in metallic thin films [2]–[5]. The acoustic dynamics of nanometre scale metallic structures have been studied in detail with pump–probe techniques in order to understand the excitation and damping dynamics of the fundamental oscillatory motion of metallic nanoparticles of different sizes and shapes [6]–[15]. In this paper, we investigate the coherent acoustic dynamics of Au nanoparticles on different substrates in order to elucidate the mechanism responsible for the decay of the acoustic excitation. In addition, we observe a strong dependence on the excited acoustic spectrum for increasing aspect ratios of the nanoparticles from a single mode spectrum to a multimode spectrum.

The Au nanostructures were fabricated by colloidal lithography, in which a monolayer of monodisperse spherical particles with 0.42–5.2 μm diameters serves as a deposition mask to produce flat Au triangles with side lengths between 120 and 1460 nm [16]. The thickness of the evaporated films ranged between 25 and 150 nm. In the first step of colloidal lithography, a 10 μl drop of colloidal suspension is placed on top of a cleaned glass or silicon substrate. Self-organization takes place due to capillary forces during the drying phase when the water evaporates. After drying, gold is thermally evaporated and finally the deposition mask is removed with adhesive tape. Figure 1(a) shows a scanning electron microscope picture close to an area where the colloids have not been removed. Figure 1(b) depicts an atomic force microscope picture of the deposited Au nanotriangles on a silicon substrate using colloids of 800 nm diameter. The triangles are clearly arranged in a hexagonal pattern with a uniform size distribution. The edge length of these triangles is 230 nm and the thickness in this case is 50 nm. For larger aspect ratios, i.e. thicker Au thickness, the shape of the triangles becomes that of a truncated pyramid.

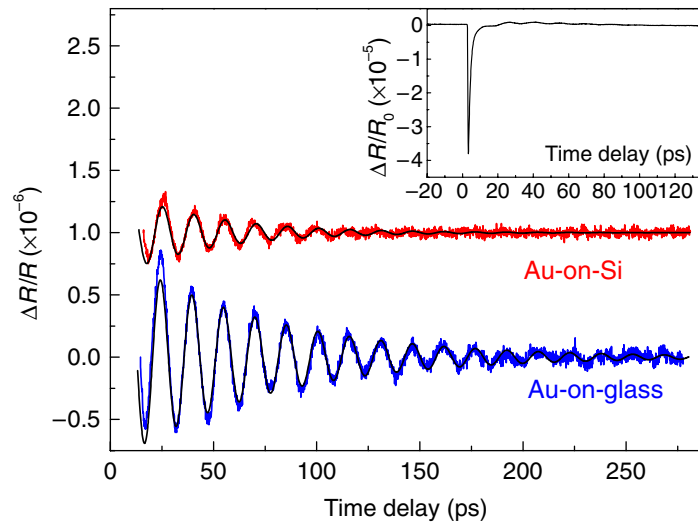


Figure 2. Oscillatory dynamics extracted from the time resolved reflectivity change of Au triangles on glass and Au triangles on silicon. The black lines are numerical fits to the data with a single frequency oscillation and mono-exponential decay. Inset: time-resolved reflectivity change of Au triangles on silicon.

Time-resolved dynamics of the nanoparticles are investigated with high-speed asynchronous optical sampling (ASOPS). High-speed ASOPS is based on two femtosecond titanium:sapphire lasers with a repetition rate around 1 GHz (Gigajet TWIN, Gigaoptics GmbH, Germany). The two lasers have a small off-set in their repetition rate in the range of 10 kHz. One of the lasers provides the pump pulses, the other the probe pulses. A 10 kHz off-set in the repetition rate allows us to scan the inverse of the repetition rate, i.e. 1 ns for 1 GHz repetition rate, within 100 μ s without any mechanical moving part in the set-up [17, 18]. The off-set frequency is stabilized electronically with a phase-locked-loop operating at the third harmonic of the repetition rate of the laser [18]. This synchronization scheme provides a timing jitter of less than 180 fs over the entire scan range of 1 ns. The high scan rate provides an efficient averaging leading to a signal-to-noise ratio better than 10^7 in a data acquisition time of 1 min. Since the system does not involve any mechanically moving part, problems encountered with mechanical delay lines like pointing instabilities and spot size variations are absent. A further advantage of the ASOPS system is the independent tunability of the two femtosecond lasers. Especially for strongly scattering samples like the ones investigated here, the pump beam can be effectively blocked in front of the detector with an edge filter. We use pump pulses at 800 nm and probe pulses at 820 nm, both with pulse durations of 50 fs. The pump and probe beams are focused on a common spot of approx. 50 μ m diameter on the samples. The average power of the pump and probe pulses is 200 and 20 mW, respectively, corresponding to energies of 200 and 20 pJ per pulse. The reflected probe beam is detected with a photo-receiver of 125 MHz bandwidth. The output of the photo-receiver is directly recorded with a 100 MS s⁻¹ 14 bit A/D converter which is triggered from the synchronization electronics of the ASOPS set-up.

The time resolved reflectivity changes of an Au-on-glass and an Au-on-silicon triangle are shown in figure 2. The triangles are both prepared with a colloid mask with 800 nm

diameter colloids, leading to triangles with an edge length of 230 nm. The thickness of the Au triangles is 25 nm. The reflectivity changes exhibit a strong negative spike at zero time delay of the order of $10^{-5} \Delta R/R_0$ due to electronic excitation of Au triangles which decays with a time constant of 1.2 ps (inset of figure 2). This time constant reflects the electronic relaxation in the Au particle. The electronic contribution is modulated by a single frequency oscillation with amplitudes in the range of $10^{-7} \Delta R/R_0$ which is extracted via subtraction of the electronic signal. The small amplitudes of the reflectivity change demonstrate the advantage of the ASOPS method to obtain a high signal-to-noise ratio in short data acquisition times over the full time delay of 1 ns. The oscillation frequency is 65.6 GHz for Au triangles on glass and 67.9 GHz on silicon, respectively, as determined from numerical fits to the data. Although the frequencies in both samples are very close to each other the damping of the acoustic oscillations differs significantly: the Au-on-glass sample exhibits an exponential decay with $\tau = 88 \pm 2$ ps, while the Au-on-Si sample is damped with $\tau = 47 \pm 2$ ps.

In thick plain metal films, i.e. with a thickness much larger than the penetration depth of the exciting laser, a strain pulse is launched by the pump pulse from the surface of the film which reappears at the surface after the roundtrip time $t_R = 2d/v_l$, with d the film thickness and v_l the longitudinal sound velocity [3, 5]. In thin films the thermal stress set-up by the pump pulse throughout the film excites the lowest thickness mode of the film which has the frequency corresponding to the inverse roundtrip time in a thick film, i.e. the observed frequency ν is given by $\nu = 1/t_R = v_l/2d$ [4]. This mode leads to a sinusoidal, single frequency modulation of the reflectivity which allows an accurate determination of the film thickness for a known sound velocity. With a sound velocity of 3280 m s^{-1} for polycrystalline Au, we can determine the thickness of the Au triangle on silicon (on glass) to be 24.1 nm (25.0 nm) from the observed frequency. The amplitude is damped through transmission of acoustic energy into the substrate. The difference in the damping times of almost a factor of two stems from the difference in the reflection coefficient at the Au–Si and Au-glass interface.

For a homogenous metallic film perfectly bonded to a substrate the reflection coefficient of an acoustic wave is determined by the acoustic impedances $Z_i = \rho_i v_{l,i}$ of the two materials, where ρ_i are the densities and $v_{l,i}$ the sound velocities. The reflection coefficient r of the acoustic amplitude is related to the acoustic impedances through

$$r = (Z_{\text{Au}} - Z_{\text{substrate}})/(Z_{\text{Au}} + Z_{\text{substrate}}). \quad (1)$$

Taking the longitudinal sound velocities of the different materials (Si along the (100) direction: 8430 m s^{-1} ; polycrystalline Au: 3280 m s^{-1} ; fused quartz: 5800 m s^{-1}) and their densities (Si 2.33 g cm^{-3} , Au 19.3 g cm^{-3} , fused quartz 2.2 g cm^{-3}) we calculate $r = 0.52$ for the Au-on-Si sample and $r = 0.66$ for the Au-on-glass sample. These values can be compared with the experimental data: the reflection coefficient is related to the frequency and the damping of the oscillations via $|r| = \exp(-1/\tau\nu)$. From our experimental data, we obtain $r_{\text{Au-Si}} = 0.73$ and $r_{\text{Au-glass}} = 0.84$. These reflectivity values are significantly larger than the theoretical ones—or in other words—the observed decay times are much too long. For perfect boundaries one would expect theoretically $\tau_{\text{Au-Si}} = 23.8 \text{ ps}$ and $\tau_{\text{Au-glass}} = 37.3 \text{ ps}$, which are both almost a factor of 2 smaller than the experimentally detected ones and far outside the uncertainty range of our experiments. We would like to note that any variations in the thickness of the Au triangles within our laser spot and thickness variations over single triangles would lead to even shorter decay times through the inhomogeneity of the associated frequencies. Hence the experimentally observed damping times are a *lower limit* for the damping of the oscillatory signal from a

single Au triangle. We would like to note that experimentally the investigation of single metallic nanoparticles has been demonstrated recently [10] which overcomes the ambiguity associated with inhomogeneous broadening. An extension of this technique using ASOPS should be possible.

The strong discrepancy between theory and experiment concerning the damping times can be resolved by assuming that the interface between the Au triangles and the substrate is not perfect. Theoretically this can be expressed through a modification of equation (1) [4]:

$$|r|^2 = [(Z_{\text{Au}} - Z_{\text{substrate}})^2 + \zeta^2] / [Z_{\text{Au}} + Z_{\text{substrate}})^2 + \zeta^2], \quad (2)$$

where $\zeta = Z_{\text{Au}}Z_{\text{Si}}\nu/\alpha$ is a frequency dependent term, with α being an effective spring constant of a massless spring describing the bonding between the Au triangle and the substrate. This massless spring model has been elaborated for multilayer systems within a transfer matrix method description by Rossignol *et al* [5]. The perfect bonding is described by $\zeta = 0$. The experimental data can be fitted with $\alpha_{\text{Au-Si}} = 1.45 \times 10^{17} \text{ g cm}^{-2} \text{ s}^{-2}$ for the Au-on-Si sample and $\alpha_{\text{Au-glass}} = 7.35 \times 10^{16} \text{ g cm}^{-2} \text{ s}^{-2}$ for the Au-on-glass sample. Our value for the Au-on-Si sample can be compared to the value of $\alpha_{\text{Au-Si}} = 1.3 \times 10^{18} \text{ g cm}^{-2} \text{ s}^{-2}$ obtained at 66 GHz for plain Au films thermally evaporated on to Si [4]. The difference in the spring constant by one order of magnitude is attributed to the difference in the preparation technique between a plain Au film on a freshly cleaned substrate and the processing steps required for colloidal lithography. In the latter the colloidal suspension is dried in ambient atmosphere which will result in a less clean surface for the subsequent Au evaporation. The influence of the surface preparation on the damping dynamics is an interesting subject for further investigations.

For nano-triangles with small aspect ratio of the thickness to the lateral dimension, we obtain the same frequencies for samples of different lateral dimensions, clearly indicating that we observe a thickness oscillation. One intriguing question is the observation of lateral or three-dimensional (3D) excitations of metallic triangles and the comparison of their damping dynamics to the damping of the thickness oscillations. The coherent excitation of lateral acoustic modes of metallic triangles have been investigated by Huang *et al* [11, 12] and Bonacina *et al* [13]. The first group investigated the dependence of the oscillation frequency of Au and Ag nano-prisms for different particle sizes on quartz substrates. In their studies a mono-mode oscillatory behavior was observed. From the size dependence of the observed frequencies they deduced the observation of an in-plane breathing motion of the particles with no dependence on the thickness of the triangles [11]. The second group investigated Ag silver plates with triangular shape in a dilute aqueous suspension [13]. They observed a bi-modal behavior. The two frequencies could be related to the two lowest-frequency lateral eigenmodes of the triangular plates.

In figure 3(a), we show ASOPS results obtained from Au triangles prepared on Si substrates with colloid diameters of 420 nm and nominal Au film thicknesses of 50, 100 and 150 nm, respectively. In this case, the edge length of the triangles is 120 nm. The time domain data reveal a complicated oscillatory structure which is reproducible at different locations of each sample. However, the overall temporal behavior of the time domain oscillations is very similar for the different samples. Multiple frequencies are observed for all samples in the numerical Fourier transform (figure 3(b)). The thickness oscillation, which would correspond to the nominal thicknesses of these films, is expected at 32.8 GHz (50 nm), 16.4 GHz (100 nm), and 10.9 GHz (150 nm), respectively. In all samples, clearly additional modes are observed. Only

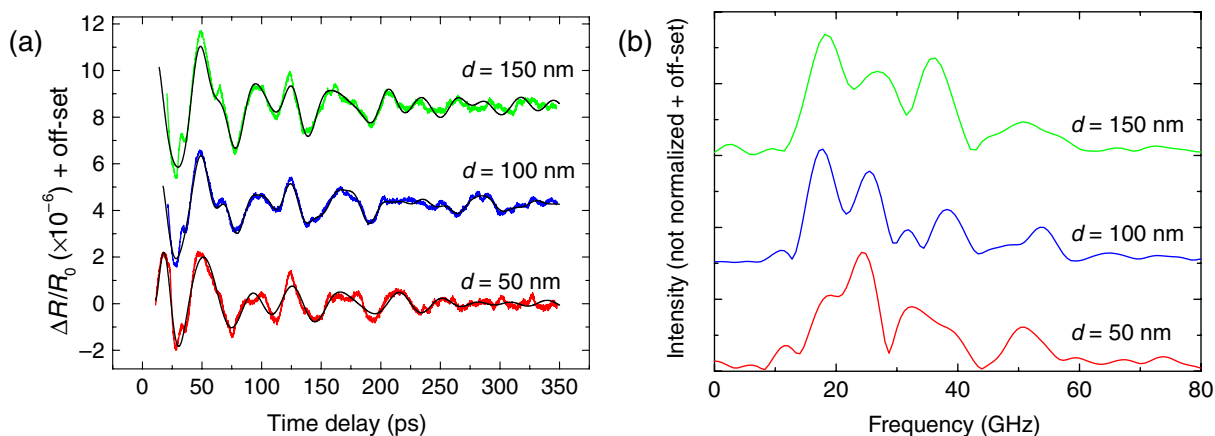


Figure 3. (a) Oscillatory traces of Au triangles prepared with 420 nm diameter colloids and 50, 100 and 150 nm nominal thicknesses, respectively. The black lines are numerical fits to the data with fit parameters as given in table 1. (b) Numerical Fourier transform of the experimental time-domain traces in (a).

the sample with 50 nm thickness exhibits a Fourier component at the expected frequency of 32.8 GHz. This Fourier component is also the strongest difference compared to the spectrum of the other two samples. The absence of a clear thickness oscillation perpendicular to the substrate for the samples with a nominal thickness of 100 and 150 nm is attributed to the shape of these samples. At large aspect ratios the shape of the nanoparticles becomes more pyramidal. Hence, the oscillation frequency for the oscillation perpendicular to the substrate is not well defined. The similarity of the spectra for different film thicknesses suggest that we observe lateral or 3D eigenmodes of different orders in the nanotriangles. We achieve very good fits to the time domain data by taking into consideration the four strongest frequency components of the Fourier spectrum for the samples with 100 and 150 nm nominal thicknesses, and five modes for the 50 nm sample (figure 3(a)). For the 100 nm and 150 nm samples the fits are very good, while for the 50 nm sample a good fit was difficult to obtain. A time-windowed Fourier transform of the experimental trace of the 50 nm sample shows indications of a non-exponential decay of certain modes which have to be investigated in more detail. The parameters of the numerical fits shown in figure 3(a) are listed in table 1. For each mode the amplitude, the frequency, the phase and the decay time of the amplitude is shown. The decay times of the coherent amplitude range from 86 to 262 ps for the 100 and 150 nm samples (7 to 278 ps for the 50 nm sample), indicating that different modes experience significantly different damping. The assignment of the frequencies to the modes of the nanoparticles and the analysis of the individual phases and damping times of each mode will help us to understand the driving forces for coherent acoustic oscillations of nanoparticles and their vibrational energy dissipation.

Our observation of a multimode spectrum differs from other observations on similar systems described above [11]–[13]. In comparison to the results reported in [11]–[13], we use excitation pulses with energies more than 4 orders of magnitude smaller. Differences in the observed spectra may result from the small fluence we use. At higher fluence larger amplitudes of the acoustic displacements are achieved. At larger amplitudes the coupling to the substrate, plasmonic coupling among nanoparticles [12,19], nonlinearities and field enhancement [20] may lead to a modification of the mode spectrum in comparison to small amplitude excitation.

Table 1. Fit parameters for the numerical fits to the data shown in figure 3(a). A_i is the amplitude, V_i the frequency, τ_i the damping constant, and φ_i the phase relative to a sine-function with phase 0 at zero time-delay.

Sample	50 nm	100 nm	150 nm
$A_1(10^{-6})$	3.42	1.29	2.15
ν_1 (GHz)	19	17.4	18.2
τ_1 (ps)	65	155	110
φ_1	-0.73	-1.98	-1.84
$A_2(10^{-6})$	2.80	1.06	1.71
ν_2 (GHz)	24.2	25.6	26.8
τ_2 (ps)	89	153	113
φ_2	-0.66	0.32	0.96
$A_3(10^{-6})$	0.35	1.03	0.770
ν_3 (GHz)	32.5	37.6	36.3
τ_3 (ps)	278	100	262
φ_3	-1.00	2.63	1.7
$A_4(10^{-6})$	20	0.444	0.656
ν_4 (GHz)	50	53.8	50.7
τ_4 (ps)	7	139	86
φ_4	-0.59	-3.23	-4.94
$A_5(10^{-6})$	40		
ν_5 (GHz)	10.3		
τ_5 (ps)	10		
φ_5	0.78		

We would like to note that we also observed a difference in the coherently excited spectrum of silica core-Au shell nanoparticles when excited with an amplified laser system and the low fluence ASOPS system [21]. For the amplified excitation the Lamb breathing mode of the Au shell dominated while the first harmonic of the thickness vibration of the shell dominated the low-fluence ASOPS data. In addition to the differences in the excitation power, the choice of the detection wavelength will also be of importance, since changes of the reflectivity close to the plasmon resonance may be affected in a different way by the different modes eventually leading to the observation of one dominant mode at high fluence excitation. These dependencies have to be investigated in more detail for the case of Au triangles and pyramids.

In conclusion, we presented a high-sensitivity method for the observation of coherent acoustic dynamics in Au triangles of different sizes on different substrates. From the experimental data, we can accurately determine the transmission and reflection coefficient of the acoustic energy at the boundary. For large aspect ratios of the triangle size to their thickness the acoustic dynamics are governed by thickness oscillations similar to those of a plain film. For smaller aspect ratio the coherent excitation of lateral modes leads to a multi-frequency oscillatory dynamic in the time domain. We expect that the ASOPS method will enable further studies of coherent acoustic dynamics in nanoparticles.

Acknowledgments

This work is supported by the Deutsche Forschungsgemeinschaft through SFB 513 and DE 567/9, and the Ministry of Science, Research and the Arts of Baden-Württemberg within the Center of Applied Photonics.

References

- [1] Cahill D G, Ford W K, Goodson K E, Mahan G D, Majumdar A, Maris H J, Merlin R and Phillpot S R 2003 *J. Appl. Phys.* **93** 793
- [2] Thomsen C, Grahn H T, Maris H J and Tauc J 1986 *Phys. Rev. B* **34** 4129
- [3] Stoner R and Maris H J 1993 *Phys. Rev. B* **48** 16373
- [4] Tas G, Loomis J J, Maris H J, Bailes A A III and Seiberling L E 1998 *Appl. Phys. Lett.* **72** 2235
- [5] Rossignol C, Perrin B, Bonello B, Djemia P, Moch P and Hurdequint H 2004 *Phys. Rev. B* **70** 094102
- [6] Perner M, Gresillon S, März J, von Plessen G, Feldmann J, Porstendorfer J, Berg K J and Berg G 2000 *Phys. Rev. Lett.* **85** 792
- [7] Antonelli G A, Maris H J, Malhota S G and Harper J M E 2002 *J. Appl. Phys.* **91** 3261
- [8] Hartland G V 2006 *Annu. Rev. Phys. Chem.* **57** 403
- [9] Arbouet A, Del Fatti N and Valleé F 2006 *J. Chem. Phys.* **124** 144701
- [10] van Dijk M A, Lippitz M and Orrit M 2005 *Phys. Rev. Lett.* **95** 267406
- [11] Huang W, Qian W and El-Sayed M A 2004 *Nano Lett.* **4** 1741
- [12] Huang W, Qian W and El-Sayed M A 2005 *J. Phys. Chem. B* **109** 18881
- [13] Bonacina L, Callegari A, Bonati C, van Mourik F and Chergui M 2006 *Nano Lett.* **6** 7
- [14] Plech A, Cerna R, Kotaidis V, Hudert F, Bartels A and Dekorsy T 2007 *Nano Lett.* **7** 1026
- [15] Petrova H *et al* 2007 *J. Chem. Phys.* **126** 094709
- [16] Burmeister F, Schäfle C, Matthes T W, Böhmisch M, Boneberg J and Leiderer P 1997 *Langmuir* **13** 2983
- [17] Bartels A, Hudert F, Janke C, Dekorsy T and Köhler K 2006 *Appl. Phys. Lett.* **88** 041117
- [18] Bartels A, Cerna R, Kistner C, Thoma A, Hudert F, Janke C and Dekorsy T 2007 *Rev. Sci. Instrum.* **78** 035107
- [19] Malikova N, Pastoriza-Santos I, Schierhorn M, Kotov N A and Liz-Marzan L M 2002 *Langmuir* **18** 3694
- [20] Leiderer P, Bartels C, Koenig-Birk J, Mosbacher M and Boneberg J 2004 *Appl. Phys. Lett.* **85** 5370
- [21] Shan X, Zhang X, Mazurenko D A, van Blaaderen A, Dijkhuis J I, Hudert F and Dekorsy T 2007 *J. Phys.: Conf. Ser. (12th Int. Conf. on Phonon Scattering in Condensed Matter)* at press